Hindawi
Discrete Dynamics in Nature and Society
Volume 2021, Article ID 5401253, 12 pages
https://doi.org/10.1155/2021/5401253

Research Article

Generalized SEIR Epidemic Model for COVID-19 in a Multipatch Environment

Lan Meng and Wei Zhu

Key Laboratory of Intelligent Analysis and Decision on Complex Systems, Chongqing University of Posts and Telecommunications, Chongqing 400065, China

Correspondence should be addressed to Wei Zhu; zhuwei@cqupt.edu.cn

Received 26 August 2021; Revised 11 November 2021; Accepted 3 December 2021; Published 17 December 2021

Academic Editor: Binxiang Dai

In this paper, an n-patch SEIR epidemic model for the coronavirus disease 2019 (COVID-19) is presented. It is shown that there is unique disease-free equilibrium for this model. Then, the dynamic behavior is studied by the basic reproduction number. The transmission of COVID-19 is fitted based on actual data. The influence of quarantined rate and population migration rate on the spread of COVID-19 is also discussed by simulation.

1. Introduction

The coronavirus disease 2019 (COVID-19) has spread to more than 200 countries worldwide, which has a significant impact on economy development, social stability, and people's daily life. According to the data on August 24, 2021, of World Health Organization, the number of confirmed cases has increased to 211,730,035 and the number of confirmed deaths cases has increased to 4,430,697 [1].

In fact, COVID-19 is one of the most serious viruses for human beings. How to reduce or control the spread of this epidemic has attracted much attention from various communities [2–8]. Zhu et al. [9] isolated COVID-19 from pneumonia patient samples and found that it belongs to the seventh member of the coronavirus family. Linton et al. [10] obtained that an average incubation period is 5 days for COVID-19 by statistical analysis of epidemic data. Chen et al. [11] presented a transmission network model and calculated the basic reproduction number of the model, which showed that COVID-19 has a higher infection rate than SARS but less than MERS. Saha et al. [12] proposed an SEIRS epidemic model to explore coronavirus infection and suggested that susceptible individuals can avoid infection by taking appropriate precautions. Quaranta et al. [13] performed a multiscale dynamic analysis of COVID-19 outbreak in Italy to show changes at different geographic scales. Leung et al. [14] established a Susceptible-Exposed-Infectious-Recovered (SEIR) model, and the basic reproduction was estimated. Based on heart rate and sleep data collected from wearables, Zhu et al. [15] proposed a framework to predict the prevalence of COVID-19 in different countries and cities. In [16], the Susceptible-Infectious-Recovered (SIR) epidemic model was proposed and explained by logistic equation. Msmali et al. [17] used a mathematical model to study the role of behavior change in slowing the spread of COVID-19 in Saudi Arabia. Hou et al. [18] investigated the urban resilience level, spatial differentiation, and dominant elements in the middle reaches of the Yangtze River under the COVID-19 pandemic. However, it is rare to establish a generalized multipatch SEIR epidemic model to study the impact of population migration and quarantine on the basic reproduction number.

With the rapid development of transportation, population migration among different regions has been one of the important factors to study the spread of epidemic. Hethcote [19] presented a model for migration between the two patches and studied the impact for migration on infectious diseases. Sattenspiel and Herring [20] presented a population flow model with n-patch and studied the dynamic behavior of the model. Driessche and Arino [21]

established an epidemic patch model for n cities and analyzed the impact of population mobility on spatial distribution. Cui et al. [22] proposed a spatial infectious disease model with migration which has the potential value for disease control. Li [23] showed that pattern transition from stationary pattern to patch invasion appears to be possible in a fully deterministic parasite-host model. Arino et al. [24] found that the possibility of disease persisting in patches and spreading epidemic increased during transportation. A two-patch SEIRS epidemic model was proposed by Liu et al. [25] to study the impact of travel on the spatial spread of dog rabies between patches with different level of disease prevalence. Zhang et al. [26] focused on a delayed multigroup SIS epidemic model with nonlinear incidence rates and patch structure. Driessche and Salmani [27] gave an SEIRS model of p-patch and analyzed the stability of the disease-free equilibrium point. The effects of heterogeneity in groups, patches, and mobility patterns on the basic reproduction number R_0 and disease prevalence were explored by Bichara et al. [28]. The dynamics of an SIS epidemic patch model with the asymmetric connectivity matrix was analyzed by Chen et al. [29], and it showed that the basic reproduction number R_0 was strictly decreasing with respect to the dispersal rate of the infected individuals. Therefore, it is necessary to study the epidemic model of multipatch. Furthermore, how to study the spread of COVID-19 in a multipatch environment is an interesting and important topic.

Inspired by above discussion, in this paper, a generalized n-patch SEIR epidemic model is formulated to study the stability of the model and the effect of control strategies on the spread of the disease. The paper is organized as follows. In Section 2, the SEIR model with n-patch for COVID-19 is proposed. In Section 3, the basic reproduction number associated with quarantined rate and population migration rate is given, and the stability of the model is studied. In Section 4, some numerical simulations are given to study the effects of migration and quarantine strategy on disease transmission. Based on the data of Hubei province, Chongqing, and Hunan province, numerical fitting is given. The numerical simulations show that appropriate quarantine strategy and control of the migration rate are important to reduce the spread of COVID-19. Conclusions are made in Section 5.

Notations: $\rho(A) \triangleq \max_{i=1,2,\ldots,n} |\lambda_i|$ and $s(A) \triangleq \max_{i=1,2,\ldots,n} \mathrm{Re}(\lambda_i)$, where $\lambda_1, \lambda_2, \ldots, \lambda_n$ are the eigenvalues of matrix A and $0_{m\times n}$ denotes the $m \times n$ zero matrix.

2. The n-Patch SEIR Model for COVID-19

The population in patch i is stratified as susceptible (S_i), exposed (E_i), infectious (I_i), quarantined (Q_i), hospitalized (H_i), and recovered (R_i). By tracing close contacts, some individuals exposed to the virus are quarantined. It is assumed that the self-quarantined susceptible individuals who stay in safe areas have no contact with infected individuals. The disease transmission in each patch is shown in Figure 1.

Based on the epidemiology of COVID-19 and the control measures taken by the government, the generalized n-patch SEIR epidemic model for COVID-19 is formulated as follows:

$$\begin{cases} \dfrac{dS_i}{dt} = b_i - \beta_i S_i (1 - z_i)(v_i E_i + I_i) - \mu_i S_i + \sum_{j\neq 1}^{n} \left(a_{ij} S_j - a_{ji} S_i\right), \\ \dfrac{dE_i}{dt} = \beta_i S_i (1 - z_i)(v_i E_i + I_i) - (q_i + \sigma_i + \mu_i) E_i + \sum_{j\neq 1}^{n} \left(b_{ij} E_j - b_{ji} E_i\right), \\ \dfrac{dI_i}{dt} = \sigma_i E_i - (\delta_i + \gamma_i + \theta_i) I_i + \sum_{j\neq 1}^{n} \left(c_{ij} I_j - c_{ji} I_i\right), \\ \dfrac{dQ_i}{dt} = q_i E_i - (\alpha_i + \mu_i) Q_i, \\ \dfrac{dH_i}{dt} = \alpha_i Q_i + \delta_i I_i - (\eta_i + g_i) H_i, \\ \dfrac{dR_i}{dt} = \gamma_i I_i + \eta_i H_i - \mu_i R_i + \sum_{j\neq 1}^{n} \left(d_{ij} R_j - d_{ji} R_i\right), \quad i = 1, 2, \ldots, n, \end{cases} \tag{1}$$

where $\beta_i, z_i, q_i, \sigma_i, \delta_i, \gamma_i$, and η_i represent the disease transmission coefficient, the self-quarantined rate of susceptible individuals, the quarantined rate of exposed individuals, the transition rate of exposed individuals to infected individuals, the transition rate of infected individuals to hospitalized individuals, the recovery rate of the infectious individuals q,

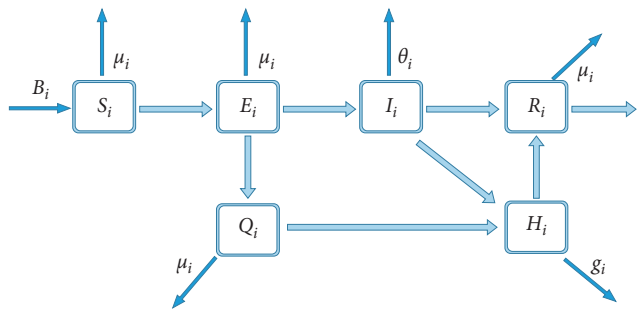

Figure 1: The disease transmission in patch i.

and the recovery rate of hospitalized individuals, respectively. Since COVID-19 differs from traditional diseases in which the exposed individuals are also infectious, the disease transmission coefficient regulator of exposed individuals v_i is added to the model. b_i, μ_i, θ_i, and g_i are the number of births per unit time, the natural death rate, the death rate of infected individuals, and the death rate of hospitalized individuals in patch i, respectively. The migration rates of susceptible, exposed individuals, infectious, and removed individuals from patch j to patch i are denoted by a_{ij}, b_{ij}, c_{ij}, and d_{ij}, respectively. It is clear that all these parameters are nonnegative.

Remark 1. Different with the model in [30], the natural birth rate, the number of births per unit time, the death rate of hospitalized individuals, and the self-quarantined rate of susceptible are taken into consideration. Moreover, people can migrate between any two patches.

3. Main Results

In order to discuss the dynamic behavior of system (1), we firstly introduce the following definition.

Definition 1 (see [31]). Let $A = [a_{ij}] \in R^{n\times n}$, where $a_{ij} < 0$ if $i \neq j$, and the sum of each column element of the matrix is positive, then the matrix is a nonsingular M matrix and $A^{-1} \geq 0$.

Lemma 1. *System (1) has unique disease-free equilibrium.*

Proof. By the definition of the disease-free equilibrium, substituting $I_i = 0$ $(i = 1, 2, \ldots, n)$ into (1), we have

$$\begin{cases} b_i - \beta_i S_i (1 - z_i) v_i E_i - \mu_i S_i + \sum_{j\neq 1}^{n} \left(a_{ij} S_j - a_{ji} S_i\right) = 0, \\ \beta_i S_i (1 - z_i) v_i E_i - (q_i + \sigma_i + \mu_i) E_i + \sum_{j\neq 1}^{n} \left(b_{ij} E_j - b_{ji} E_i\right) = 0, \\ \sigma_i E_i = 0, \\ q_i E_i - (\alpha_i + \mu_i) Q_i = 0, \\ \alpha_i Q_i - (\eta_i + g_i) H_i = 0, \\ \eta_i H_i - \mu_i R_i + \sum_{j\neq 1}^{n} \left(d_{ij} R_j - d_{ji} R_i\right) = 0, \quad i = 1, 2, \ldots, n. \end{cases} \tag{2}$$

Then,

$$\begin{cases} b_i - \mu_i S_i + \sum_{j=1}^{n} \left(a_{ij} S_j - a_{ji} S_i\right) = 0, \\ -\mu_i R_i + \sum_{j\neq 1}^{n} \left(d_{ij} R_j - d_{ji} R_i\right) = 0, \quad i = 1, 2, \ldots, n, \end{cases} \tag{3}$$

that is,

$$\begin{cases} G_1 S = B, \\ G_2 R = \mathbf{0}, \end{cases} \tag{4}$$

where

$$\begin{aligned} S &= (S_1, S_2, \ldots, S_n)', \\ B &= (B_1, B_2, \ldots, B_n)', \\ R &= (R_1, R_2, \ldots, R_n), \\ \mathbf{0} &= 0_{n\times 1}, \end{aligned}$$

$$G_1 = \begin{bmatrix} \mu_1 + \sum_{j\neq 1}^{n} a_{j1} & -a_{12} & \cdots & -a_{1n} \\ -a_{21} & \mu_2 + \sum_{j\neq 2}^{n} a_{j2} & \cdots & -a_{2n} \\ \vdots & \vdots & \ddots & \vdots \\ -a_{n1} & -a_{n2} & \cdots & \mu_n + \sum_{j\neq n}^{n} a_{jn} \end{bmatrix},$$
$$G_2 = \begin{bmatrix} \mu_1 + \sum_{j\neq 1}^{n} d_{j1} & -d_{12} & \cdots & -d_{1n} \\ -d_{21} & \mu_2 + \sum_{j\neq 2}^{n} d_{j2} & \cdots & -d_{2n} \\ \vdots & \vdots & \ddots & \vdots \\ -d_{n1} & -d_{n2} & \cdots & \mu_n + \sum_{j\neq n}^{n} d_{jn} \end{bmatrix}. \tag{5}$$

Since G_1 and G_2 are nonsingular M-matrix, then $G_1^{-1} \geq 0$ and $G_2^{-1} \geq 0$. Therefore, (3) has unique solution $S^* = (S_1^0, S_2^0, \ldots, S_n^0)' = G_1^{-1}B$ and $R^* = \mathbf{0}$.

Thus, system (1) has unique disease-free equilibrium $C_0 = (S^{*\prime}, 0', 0', 0', 0', 0')$.

The proof is completed. □

Lemma 2. *$\Gamma = (S_1, E_1, I_1, Q_1, H_1, R_1, \ldots, S_n, E_n, I_n, Q_n, H_n, R_n) \in \mathbb{R}_+^{6n} | N(t) \leq (\overline{B}/\mu^*)$, $0 \leq S_i \leq S_i^0, i = 1, 2, \ldots, n$, is a positively invariant set for system (1), where $\overline{B} = \sum_{i=1}^{n} b_i, \mu^* = \min\{\mu_i, \theta_i, g_i\}$ and $N(t) = \sum_{i=1}^{n} (S_i + E_i + I_i + Q_i + H_i + R_i)$.*

Proof. In term of system (1), we have

$$\begin{aligned} \dot{N}(t) &= \overline{B} - \sum_{i=1}^{n} (\mu_i S_i + \mu_i E_i + \theta_i I_i + \mu_i Q_i + g_i H_i + \mu_i R_i) + \\ &\sum_{i=1}^{n} \left[\sum_{j=1}^{n} (a_{ij} S_j - a_{ji} S_i) + \sum_{j=1}^{n} (b_{ij} E_j - b_{ji} E_i) + \sum_{j=1}^{n} (c_{ij} I_j - c_{ji} I_i) \right. \\ &\left. + \sum_{j=1}^{n} (d_{ij} R_j - d_{ji} R_i) \right] \\ &= \overline{B} - \sum_{i=1}^{n} (\mu_i S_i + \mu_i E_i + \theta_i I_i + \mu_i Q_i + g_i H_i + \mu_i R_i) \leq \overline{B} - \mu^* N. \end{aligned} \tag{6}$$

Therefore,

$$N(t) \leq \left(N(0) - \frac{\overline{B}}{\mu^*} \right) e^{-\mu^* t} + \frac{\overline{B}}{\mu^*}, \tag{7}$$

where $N(0)$ is the initial population.

Therefore, $N(t) \leq \overline{B}/\mu^*$ if and only if $N(0) \leq \overline{B}/\mu^*$.

From the first equation of system (1), we have

$$\frac{dS_i}{dt} \leq b_i - \mu_i S_i + \sum_{j=1}^{n} (a_{ij} S_j - a_{ji} S_i) = (G_1 S^0 - G_1 S)_i, \tag{8}$$

where $(G_1 S^0 - G_1 S)_i$ is the i-th element of $G_1 S^0 - G_1 S$.

Therefore, $dS_i/dt \leq 0$ if $S_i = S_i^0, S_j \leq S_j^0$, $i, j = 1, 2, \ldots, n$, and $i \neq j$.

The proof is completed.

Based on Lemma 2, the dynamical properties of system (1) are studied only in Γ. Now, we are in the position to discuss the basic reproduction number of system (1).

Define $F = \begin{bmatrix} F_{11} & F_{12} \\ 0 & 0 \end{bmatrix}$ and $V = \begin{bmatrix} V_{11} & 0 \\ V_{21} & V_{22} \end{bmatrix}$, where

$$
\begin{aligned}
F_{11} &= \operatorname{diag}(v_1', v_2', \ldots, v_n'), \quad v_i' = (1 - z_i)\beta_i v_i S_i^0, \\
F_{12} &= \operatorname{diag}(u_1, u_2, \ldots, u_n), \quad u_i = (1 - z_i)\beta_i S_i^0, \\
V_{11} &= \begin{bmatrix}
(q_1 + \sigma_1 + \mu_1) + \sum_{j\neq 1}^{n} b_{j1} & -b_{12} & \cdots & -b_{1n} \\
-b_{21} & (q_2 + \sigma_2 + \mu_2) + \sum_{j\neq 2}^{n} b_{j2} & \cdots & -b_{2n} \\
\vdots & \vdots & \ddots & \vdots \\
-b_{n1} & -b_{n2} & \cdots & (q_n + \sigma_n + \mu_n) + \sum_{j\neq n}^{n} b_{jn}
\end{bmatrix}, \\
V_{21} &= \operatorname{diag}(-\sigma_1, -\sigma_2, \ldots, -\sigma_n), \\
V_{22} &= \begin{bmatrix}
(\delta_1 + \gamma_1 + \theta_1) + \sum_{j\neq 1}^{n} c_{j1} & -c_{12} & \cdots & -c_{1n} \\
-c_{21} & (\delta_2 + \gamma_1 + \theta_1) + \sum_{j\neq 2}^{n} c_{j2} & \cdots & -c_{2n} \\
\vdots & \vdots & \ddots & \vdots \\
-c_{n1} & -c_{n2} & \cdots & (\delta_n + \gamma_n + \theta_n) + \sum_{j\neq n}^{n} c_{jn}
\end{bmatrix}.
\end{aligned}
\tag{9}
$$

By using the method in Driessche and Watmough [31], the basic reproduction number R_0 can be determined by computing the spectral radius of the matrix as follows:

$$
FV^{-1} = \begin{bmatrix} F_{11}V_{11}^{-1} - F_{12}V_{22}^{-1}V_{21}V_{11}^{-1} & F_{12}V_{22}^{-1} \\ 0 & 0 \end{bmatrix}, \tag{10}
$$

that is, $R_0 = \rho(FV^{-1}) = \rho(F_{11}V_{11}^{-1} - F_{12}V_{11}^{-1}V_{21}V_{22}^{-1})$. □

Lemma 3 (see [32]). *If J_1 is a nonnegative matrix and J_2 is a nonsingular matrix, then $s(J_1 - J_2) < 0 \Leftrightarrow \rho(J_1 J_2^{-1}) < 1$ and $s(J_1 - J_2) > 0 \Leftrightarrow \rho(J_1 J_2^{-1}) > 1$.*

Theorem 1. *The disease-free equilibrium C_0 is globally asymptotically stable if $R_0 < 1$, and the disease-free equilibrium C_0 is unstable if $R_0 > 1$.*

$$
\dot{X} = (F - V)X. \tag{11}
$$

Proof. From the second equations and the third equations of system (1), we have, that is, $X = (E_1, E_2, \ldots, E_n, I_1, I_2, \ldots, I_n)'$.

Since F is a nonnegative matrix and V is a nonsingular matrix, it follows from Lemma 3 that

$$
S(F - V) > 0, \quad \text{if } R_0 = \rho\left(FV^{-1}\right) > 1. \tag{12}
$$

Thus, the disease-free equilibrium C_0 is unstable if $R_0 > 1$.

Next, we prove C_0 is globally asymptotically stable if $R_0 < 1$.

Since

$$
V^{-1}F = V^{-1}FV^{-1}V, \tag{13}
$$

then $V^{-1}F$ is similar to FV^{-1}. Therefore,

$$
\rho\left(V^{-1}F\right) = \rho\left(FV^{-1}\right) = R_0. \tag{14}
$$

Since $V^{-1}F$ is a nonnegative irreducible matrix, by Perron–Frobenius theorem [31], $V^{-1}F$ has a positive left eigenvector x and

$$
x\left(V^{-1}F\right) = \rho\left(FV^{-1}\right)x. \tag{15}
$$

Let $x = (e_1, e_2, \ldots, e_n, r_1, r_2, \ldots, r_n)$, then

$$
\begin{aligned}
&(e_1, e_2, \ldots, e_n, r_1, r_2, \ldots, r_n)\, V^{-1} \\
&F = R_0\, (e_1, e_2, \ldots, e_n, r_1, r_2, \ldots, r_n).
\end{aligned}
\tag{16}
$$

Let $W = \sum_{i=1}^{n} k_i E_i + \sum_{i=1}^{n} l_i I_i$ be a candidate Lyapunov function, where

$$
(k_1, k_2, \ldots, k_n, l_1, l_2, \ldots, l_n) = (e_1, e_2, \ldots, e_n, r_1, r_2, \ldots, r_n)V^{-1}. \tag{17}
$$

Then, calculating the derivative of W along the solution of system (1), we have

Table 1: Parameter data and sources of Hubei province, Chongqing, and Hunan province, China.

	$i=1$	$i=2$	$i=3$	Average error	Source
β_i	2×10^{-9}	2×10^{-10}	8.2×10^{-11}	3.2×10^{-11}	LSE
ν_i	1.8	1.5	1.6	0.13	LSE
σ_i	0.2	0.2	0.2	—	[10]
μ_i	1.94×10^{-5}	3.62×10^{-5}	2×10^{-5}	—	[33–35]
γ_i	0.005	0.005	0.005	—	[36–38]
θ_i	0.01	0.01	0.01	—	[36–38]
g_i	0.004	0.0005	0.0002	—	[36–38]
b_i	1841	1126	1967	—	[33–35]
η_i	0.024	0.043	0.055	—	[36–38]
$S_i(0)$	59270000	3254200	73195300	—	[33–35]
$E_i(0)$	28000	320	750	323	LSE
$I_i(0)$	14500	160	310	217	LSE
$Q_i(0)$	2000	60	120	113	LSE
$H_i(0)$	958	75	69	—	[36–38]
$R_i(0)$	42	0	0	—	[36–38]
q_i^1	0.15	0.03	0.02	0.005	LSE
z_i^1	0.53	0.62	0.5	0.08	LSE
δ_i^1	0.04	0.12	0.15	0.02	LSE
α_i^1	0.07	0.11	0.01	0.01	LSE
q_i^2	0.85	0.86	0.78	0.05	LSE
z_i^2	0.87	0.85	0.8	0.09	LSE
δ_i^2	0.17	0.25	0.4	0.07	LSE
α_i^2	0.005	0.08	0.002	0.004	LSE

$$
\begin{aligned}
\dot{W} &= \sum_{i=1}^{n}\left(k_i\frac{\mathrm{d}E_i}{\mathrm{d}t}+l_i\frac{\mathrm{d}I_i}{\mathrm{d}t}\right)\\
&= \sum_{i=1}^{n}k_i\left[\beta_iS_i(1-z_i)(\nu_iE_i+I_i)-(q_i+\sigma_i+\mu_i)E_i+\sum_{j=1}^{n}\left(b_{ij}E_j-b_{ji}E_i\right)\right]\\
&\quad+\sum_{i=1}^{n}l_i\left[\sigma_iE_i-(\delta_i+\gamma_i+\theta_i)I_i+\sum_{j=1}^{n}\left(c_{ij}I_j-c_{ji}I_i\right)\right]\\
&\le \sum_{i=1}^{n}k_i\left[\beta_iS_i^0(1-z_i)(\nu_iE_i+I_i)-(q_i+\sigma_i+\mu_i)E_i+\sum_{j=1}^{n}\left(b_{ij}E_j-b_{ji}E_i\right)\right]\\
&\quad+\sum_{i=1}^{n}l_i\left[\sigma_iE_i-(\delta_i+\gamma_i+\theta_i)I_i+\sum_{j=1}^{n}\left(c_{ij}I_j-c_{ji}I_i\right)\right]\\
&= (k_1,k_2,\ldots,k_n)[(F_{11}-V_{11})E+F_{12}I]-(l_1,l_2,\ldots,l_n)(V_{21}E+V_{22}I)\\
&= (k_1,k_2,\ldots,k_n,l_1,l_2,\ldots,l_n)(F-V)X\\
&= (e_1,e_2,\ldots,e_n,r_1,r_2,\ldots,r_n)V^{-1}(F-V)X\\
&= (e_1,e_2,\ldots,e_n,r_1,r_2,\ldots,r_n)\left(V^{-1}F-E\right)X\\
&= (e_1,e_2,\ldots,e_n,r_1,r_2,\ldots,r_n)(R_0-1)X,
\end{aligned}
\tag{18}
$$

where $E=(E_1,E_2,\ldots,E_n)'$ and $I=(I_1,I_2,\ldots,I_n)'$.

If $R_0 < 1$, then $\dot{W} \le 0$, and $\dot{W} = 0$ if and only if $S_i = S_i^0$ or $E_i = 0$, $I_i = 0$, $i = 1, 2, \ldots, n$.

Thus, C_0 is globally asymptotically stable if $R_0 < 1$.

The proof is completed. □

4. Numerical Simulation of COVID-19 Transmission

In this section, the spread of COVID-19 among Hubei province, Chongqing, and Hunan province is simulated. The SEIR epidemic model with $n = 3$ is restated is as follows:

$$\begin{cases} \dfrac{dS_i}{dt} = b_i - \beta_i S_i (1 - z_i)(v_i E_i + I_i) - \mu_i S_i + \sum_{j \neq 1}^{n} \left(a_{ij} S_j - a_{ji} S_i\right), \\ \dfrac{dE_i}{dt} = \beta_i S_i (1 - z_i)(v_i E_i + I_i) - (q_i + \sigma_i + \mu_i) E_i + \sum_{j \neq 1}^{n} \left(b_{ij} E_j - b_{ji} E_i\right), \\ \dfrac{dI_i}{dt} = \sigma_i E_i - (\delta_i + \gamma_i + \theta_i) I_i + \sum_{j \neq 1}^{n} \left(c_{ij} I_j - c_{ji} I_i\right), \\ \dfrac{dQ_i}{dt} = q_i E_i - (\alpha_i + \mu_i) Q_i, \\ \dfrac{dH_i}{dt} = \alpha_i Q_i + \delta_i I_i - (\eta_i + g_i) H_i, \\ \dfrac{dR_i}{dt} = \gamma_i I_i + \eta_i H_i - \mu_i R_i + \sum_{j \neq 1}^{n} \left(d_{ij} R_j - d_{ji} R_i\right), \quad i = 1, 2, \ldots, n. \end{cases} \tag{19}$$

It is assumed that $a_{ij} = b_{ij} = c_{ij} = d_{ij} = p_{ij}$, i, $j = 1, 2, 3$, and $i \neq j$, where p_{ij} is the migration rate from patch j to patch i. The migration matrix is $P = (p_{ij})_{3\times 3}$, where $p_{ii} = 0$, $i = 1, 2, 3$.

4.1. Fitting on the Transmission of COVID-19. Let $i = 1, 2$, and 3 represent Hubei province, Chongqing, and Hunan province in system (19), respectively. The values of θ_i and γ_i are taken as the average death rate and cure rate of confirmed infected persons in patch i from January 20, 2020, to February 1, 2020. The values of g_i and η_i are taken as the average death rate and cure rate of confirmed infected persons in patch i from January 25, 2020, to March 1, 2020, respectively. Based on the data from January 25, 2020, to March 15, 2020, least squares estimate (LSE) is used to estimate the parameters. The data are divided into two stages: the first stage is from January 25 to February 7 and the second stage is from February 8 to March 15, 2020. The difference between the two stages is reflected in q_i, z_i, δ_i, and α_i. Moreover, q_i^j, z_i^j, δ_i^j, and α_i^j represent the corresponding parameter value of the j-th stage, where $j = 1, 2$. The parameters of system (19) are shown in Table 1.

The numerical fitting diagram is shown in Figure 2. It can be found that the simulated curve is approximately the same as the actual data.

4.2. The Effects of Migration and Quarantine Measures on COVID-19 Transmission. Next, the effect of migration on COVID-19 transmission is shown in Figure 3 when only migration rate is changed. As the migration rate increases, the number of cumulative confirmed cases increases in Chongqing and Hunan province. However, with the increase in migration rate, the number of cumulative confirmed cases decreases in Hubei province. In this case, since the epidemic situation is most severe in Hubei province, population migration can reduce the spread of COVID-19 in Hubei province. Nevertheless, it makes epidemic situation worse in other areas.

The effect of quarantine strategy on COVID-19 transmission is shown in Figure 4 when only quarantined rate is changed. Figures 4(a)–4(c) show that if quarantine measures had not been implemented, the epidemic situation would have been worse than the actual situation, especially in Hubei province. Furthermore, as the quarantined rate increases, the

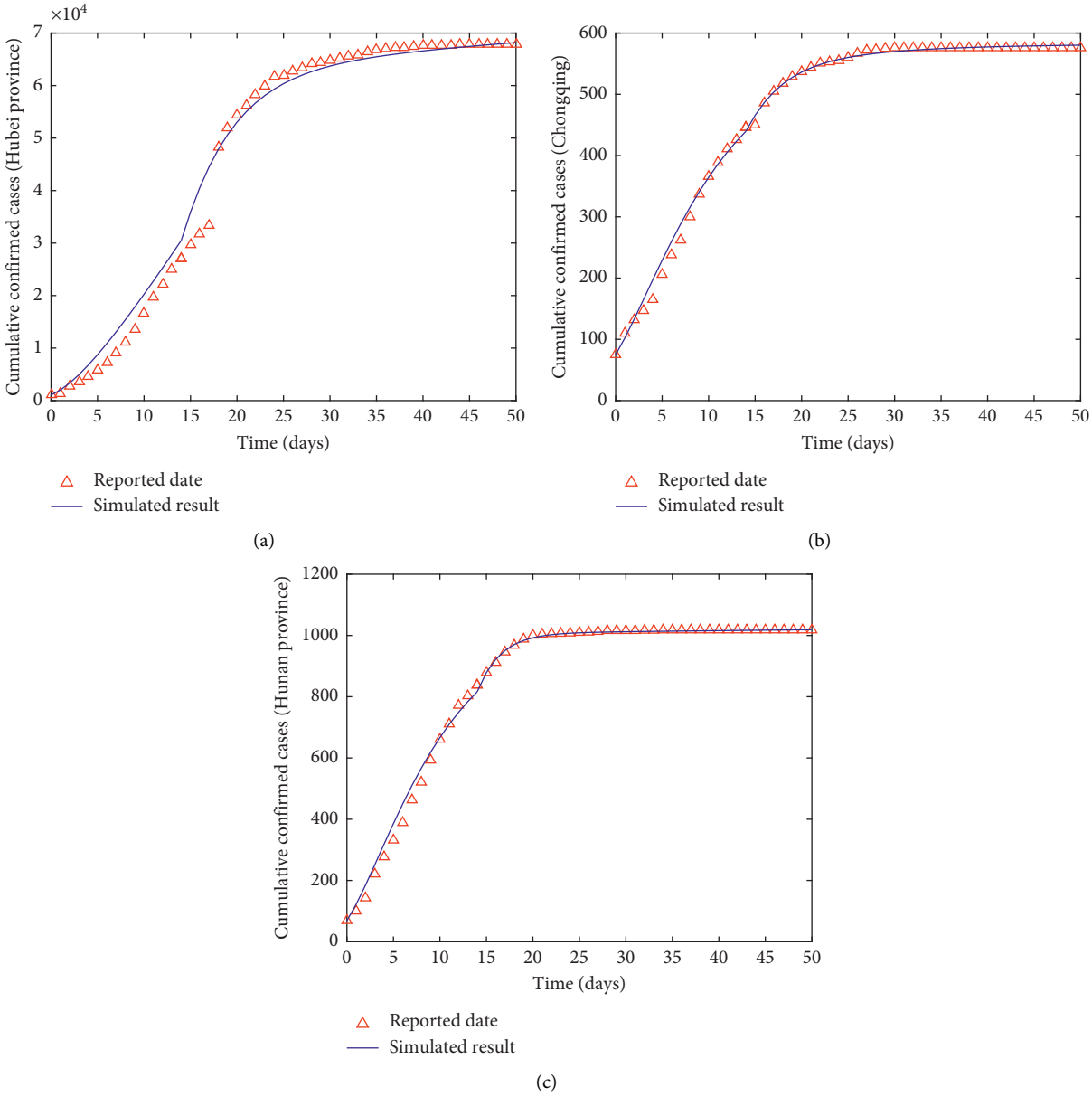

Figure 2: Fitting on the transmission of COVID-19 in (a) Hubei province; (b) Chongqing; (c) Hunan province.

number of cumulative confirmed cases will decrease. In Figure 4(d), the red solid represents self-quarantined rate of susceptible individuals where $P = P_0, z_i = 0,$ and $i = 1, 2, 3$; black solid represents quarantined rate of exposed individuals where $P = P_0, q_i = 0,$ and $i = 1, 2, 3$; and blue solid represents that both kinds of quarantine strategies are performed simultaneously where $P = P_0, q_i = z_i,$ and $i = 1, 2, 3$. Figure 4(d) shows that R_0 decreases with the increase in quarantined rate. The simultaneous execution of both quarantine strategies has the greatest impact on R_0. Therefore, quarantine strategy plays an important and effective role in controlling the outbreak. Thus, reducing migration rate and increasing quarantine measures in Hubei can effectively reduce the spread of the disease.

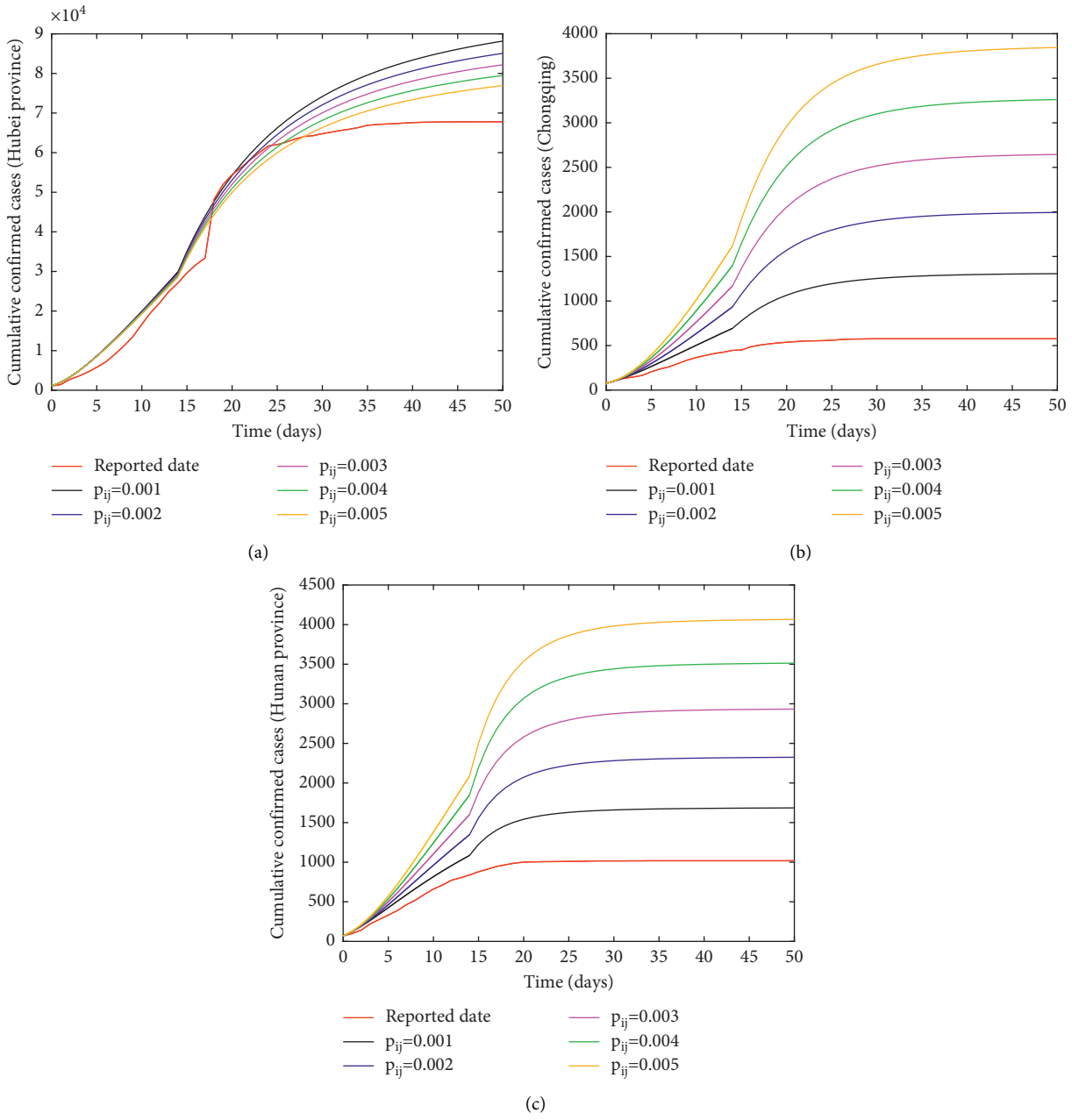

Figure 3: Effect of migration rate on COVID-19 transmission, where $i, j = 1, 2, 3$: (a) Hubei province; (b) Chongqing; (c) Hunan province.

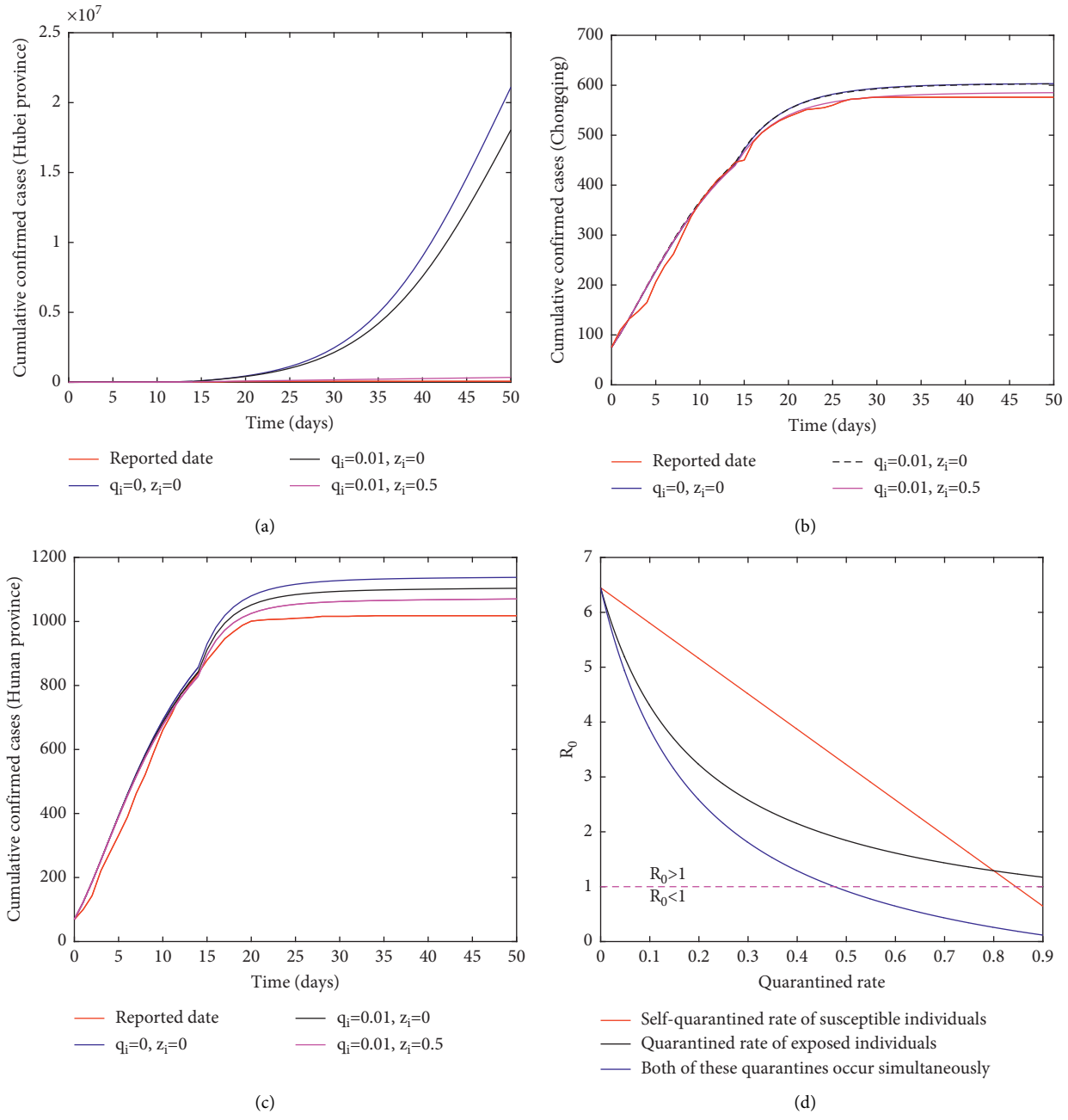

FIGURE 4: Effect of quarantined rate on COVID-19 transmission, where $i = 1, 2, 3$: (a) Hubei province; (b) Chongqing; (c) Hunan province.

5. Conclusion

In this paper, based on epidemiological characteristics of COVID-19 and government intervention strategy, an n-patch SEIR epidemic model is presented. It is shown that system (1) has unique disease-free equilibrium C_0. Moreover, C_0 is globally asymptotically stable $R_0 < 1$, and it is unstable if $R_0 > 1$. A 3-patch SEIR epidemic model is formulated to explore the effect of migration rate and quarantined rate on COVID-19 transmission. The numerical results show that appropriate controls on migration and quarantined rate are necessary to prevent outbreaks.

Data Availability

The data are available on Hubei Provincial Bureau of Statistics website, Chongqing Bureau of Statistics website, Hunan Provincial Bureau of Statistics website, Health Commission of Hubei Province website, Health Commission of Chongqing website, and Health Commission of Hunan Province website. Detailed links are given in references.

Conflicts of Interest

The authors declare that they have no conflicts of interest.

Acknowledgments

This work was supported partly by National Natural Science Foundation of China under Grants 61673080, 61773321, and 61773083, partly by the Science and Technology Research Program of Chongqing Municipal Education Commission under Grant KJZD-K202000601, partly by Natural Science Foundation of Chongqing under Grant cstc2019jcyj-msxmX0102, and partly by Venture & Innovation Support Program for Chongqing Overseas Returnees under Grant cx2017099.

References

[1] World Health Organization (WHO), *Coronavirus Disease (COVID-19) Pandemic*, Geneva, Switzerland, 2019, https://www.who.int/emergencies/diseases/novel-coronavirus-2019.

[2] J. F.-W. Chan, S. Yuan, K.-H. Kok et al., "A familial cluster of pneumonia associated with the 2019 novel coronavirus indicating person-to-person transmission: a study of a family cluster," *The Lancet*, vol. 395, no. 10223, pp. 514–523, 2020.

[3] M. U. G. Kraemer, C.-H. Yang, B. Gutierrez et al., "The effect of human mobility and control measures on the COVID-19 epidemic in China," *Science*, vol. 368, no. 6490, pp. 493–497, 2020.

[4] B. Tang, X. Wang, Q. Li et al., "Estimation of the transmission risk of the 2019-nCoV and its implication for public Health interventions," *Journal of Clinical Medicine*, vol. 9, no. 2, p. 462, 2020.

[5] B. Tang, N. L. Bragazzi, Q. Li, S. Tang, Y. Xiao, and J. Wu, "An updated estimation of the risk of transmission of the novel coronavirus (2019-nCov)," *Infectious Disease Modelling*, vol. 5, no. 1, pp. 248–255, 2020.

[6] Y. Chen, J. Cheng, and Y. Liu, "A time delay dynamic system with external source for the local outbreak of 2019-nCoV," *Applicable Analysis*, vol. 50, no. 3, pp. 1–12, 2020.

[7] O. Khyar and K. Allali, "Global dynamics of a multi-strain SEIR epidemic model with general incidence rates: application to COVID-19 pandemic," *Nonlinear Dynamics*, vol. 102, no. 1, pp. 489–509, 2020.

[8] W. Li, J. Zhou, and J.-A. Lu, "The effect of behavior of wearing masks on epidemic dynamics," *Nonlinear Dynamics*, vol. 101, no. 3, pp. 1995–2001, 2020.

[9] N. Zhu, D. Zhang, W. Wang et al., "A novel coronavirus from patients with pneumonia in China, 2019," *New England Journal of Medicine*, vol. 382, no. 8, pp. 727–733, 2020.

[10] N. M. Linton, T. Kobayashi, Y. C. Yang et al., "Incubation period and other epidemiological characteristics of 2019 novel coronavirus infections with right truncation: a statistical analysis of publicly available case data," *MedRxiv*, vol. 9, no. 2, 538 pages, 2020.

[11] T. M. Chen, J. Rui, Q. P. Wang, Z. Y. Zhao, J. A. Cui, and L. Yin, "A mathematical model for simulating the phase-based transmissibility of a novel coronavirus," *Infectious Diseases of Poverty*, vol. 9, no. 1, pp. 18–25, 2020.

[12] S. Saha, G. P. Samanta, and J. J. Nieto, "Epidemic model of COVID-19 outbreak by inducing behavioural response in population," *Nonlinear Dynamics*, vol. 102, no. 1, pp. 455–487, 2020.

[13] G. Quaranta, G. Formica, J. T. Machado, W. Lacarbonara, and S. F. Masri, "Understanding COVID-19 nonlinear multi-scale dynamic spreading in Italy," *Nonlinear Dynamics*, vol. 101, no. 3, pp. 1583–1619, 2020.

[14] K. Leung, J. T. Wu, and G. M. Leung, "Nowcasting and forecasting the potential domestic and international spread of the 2019-nCoV outbreak originating in Wuhan, China: a modelling study," *Lancet*, vol. 395, no. 10225, pp. 689–697, 2020.

[15] G. Zhu, J. Li, Z. Meng et al., "Learning from large-scale wearable device data for predicting the epidemic trend of COVID-19," *Discrete Dynamics in Nature and Society*, vol. 2020, Article ID 6152041, 8 pages, 2020.

[16] M. De la Sen and A. Ibeas, "On an sir epidemic model for the COVID-19 pandemic and the logistic equation," *Discrete Dynamics in Nature and Society*, vol. 2020, no. 3, 17 pages, Article ID 1382870, 2020.

[17] A. Msmali, M. Zico, I. Mechai, and A. Ahmadini, "Modeling and simulation: a study on predicting the outbreak of COVID-19 in Saudi Arabia," *Discrete Dynamics in Nature and Society*, vol. 2021, no. 6, 19 pages, Article ID 5522928, 2021.

[18] X. Hou, Q. Ma, and X. Wang, "Spatial differentiation and elements influencing urban resilience in the middle reaches of the Yangtze River under the COVID-19 pandemic," *Discrete Dynamics in Nature and Society*, vol. 2021, no. 19, 18 pages, Article ID 6687869, 2021.

[19] H. W. Hethcote, "Qualitative analyses of communicable disease models," *Mathematical Bioences*, vol. 28, no. 3-4, pp. 335–356, 1976.

[20] L. Sattenspiel and D. A. Herring, "Structured epidemic models and the spread of influenza in the central Canadian subarctic," *Human Biology*, vol. 70, no. 1, pp. 91–115, 1998.

[21] P. V. D. Driessche and J. Arino, "A multi-city epidemic model," *Mathematical Population Studies*, vol. 10, pp. 175–193, 2003.

[22] M. Cui, T.-H. Ma, and X.-E. Li, "Spatial behavior of an epidemic model with migration," *Nonlinear Dynamics*, vol. 64, no. 4, pp. 331–338, 2011.

[23] L. Li, "Patch invasion in a spatial epidemic model," *Applied Mathematics and Computation*, vol. 258, pp. 342–349, 2015.

[24] J. Arino, C. Sun, and W. Yang, "Revisiting a two-patch SIS model with infection during transport," *Mathematical Medicine and Biology*, vol. 33, no. 1, pp. 29–55, 2015.

[25] J. Liu, Y. Jia, and T. Zhang, "Analysis of a rabies transmission model with population dispersal," *Nonlinear Analysis: Real World Applications*, vol. 35, pp. 229–249, 2017.

[26] H. Zhang, J. Xia, and P. Georgescu, "Multigroup deterministic and stochastic SEIRI epidemic models with nonlinear incidence rates and distributed delays: a stability analysis," *Mathematical Methods in the Applied Sciences*, vol. 40, no. 18, pp. 6254–6275, 2017.

[27] P. V. D. Driessche and M. Salmani, "A model for disease transmission in a patchy environment," *Discrete and Continuous Dynamical Systems*, vol. 6, no. 1, pp. 185–202, 2017.

[28] D. Bichara and A. Iggidr, "Multi-patch and multi-group epidemic models: a new framework," *Journal of Mathematical Biology*, vol. 77, no. 1, pp. 107–134, 2018.

[29] S. Chen, J. Shi, Z. Shuai, and Y. Wu, "Asymptotic profiles of the steady states for an SIS epidemic patch model with asymmetric connectivity matrix," *Journal of Mathematical Biology*, vol. 80, no. 7, pp. 2327–2361, 2020.

[30] X. Wang, S. Tang, Y. Chen, X. Yanni, and F. Xiamoei, "When will be the resumption of work in Wuhan and its surrounding areas during COVID-19 epidemic? A data-driven network modeling analysis," *Scientia Sinica Mathematica*, vol. 50, pp. 1–10, 2020.

[31] A. Berman and R. J. Plemmons, "Nonnegative matrices in the mathematical sciences," *Society for Industrial and Applied Mathematics*, vol. 150, pp. 55–66, 1979.
[32] P. V. D. Driessche and M. Salmani, "A model for disease transmission in a patchy environment," *Discrete and Continuous Dynamical Systems*, vol. 6, no. 1, pp. 185–202, 2006.
[33] Hubei Provincial Bureau of Statistics: http://tjj.hubei.gov.cn/tjsj/sjkscx/tjnj/qstjnj/, 2021.
[34] Chongqing Bureau of Statistics: http://tjj.cq.gov.cn/zwgk_233/tjnj/, 2021.
[35] Hunan Provincial Bureau of Statistics: http://tjj.hunan.gov.cn/hntj/tjsj/tjnj/index.html, 2021.
[36] Health Commission of Hubei Province, *Novel Coronavirus Situation Report of Hubei Province*, Health Commission of Hubei Province, Hubei, China, 2021, http://wjw.hubei.gov.cn/bmdt/ztzl/fkxxgzbdgrfyyq/xxfb/.
[37] Health Commission of Chongqing, *Novel Coronavirus Situation Report of Chongqing*, Health Commission of Chongqing, Chongqing, China, 2021, http://wsjkw.cq.gov.cn/ztzl_242/qlzhxxgzbdfyyqfkgz/yqtb/.
[38] Health Commission of Hunan Province, *Novel Coronavirus Situation Report of Hunan Province*, Health Commission of Hunan Province, Hunan, China, 2021, http://wjw.hunan.gov.cn/wjw/qwfb/yqfkgz_list_25.html.